Journal of Materials Chemistry B

Accepted Manuscript

ROYAL SOCIETY OF CHEMISTRY

www.rsc.org/materialsB

Cite this: DOI: 10.1039/c0xx00000x

www.rsc.org/xxxxxx

ARTICLE TYPE

A Reusable Ratiometric Two-Photon Chemodosimeter for Hg^{2+} based on ESIPT and Its Application in Bioimaging

Weifang Luo, Huie Jiang, Kaiming Zhang, Wei Liu, Xiaoliang Tang, Wei Dou, Zhenghua Ju, Zhiqi Li and Weisheng Liu*

Received (in XXX, XXX) Xth XXXXXXXXX 20XX, Accepted Xth XXXXXXXXX 20XX
DOI: 10.1039/b000000x

A novel ratiometric fluorescence chemodosimeter has been developed for reusable detection of Hg^{2+}. The chemodosimeter responds to Hg^{2+} sensitively and selectively with remarkably fluorescent change from green to blue through hampering the excited state intramolecular proton transfer (ESIPT) process. This recyclable chemodosimeter can remove Hg^{2+} from water by forming a unique mercury-containing compound, which could be reused in the presence of $NaBH_4$. Moreover, the chemodosimeter exhibits a ratiometric fluorescence response towards Hg^{2+} with a very low detection limit (1.0 ppb), and it can be used to detect Hg^{2+} in drinking water. Furthermore, the ratiometric chemodosimeter has been successfully used to the imaging of Hg^{2+} in living cells and tissues with two-photon fluorescence microscopy due to the remarkable emission change from green to blue. This provides a novel testing method for detecting Hg^{2+} in living cells and tissues with low cytotoxicity and autofluorescence.

1. Introduction

Detecting mercury ion has received considerable attention owing to its extremely toxic impact on the environment and human health. The accumulation of mercury ion in human body can lead to permanent deterioration of the central nervous and endocrine system because the ion passes easily through biological membranes, such as skin, respiratory and gastrointestinal tissues.[1, 2] Hg^{2+} is widely distributed in air, water and soil, which can be recognizable even at very low concentrations.[3-5] The U.S. Environmental Protection Agency (EPA) has set the limit of mercury in drinking water to be 2 ppb.[6] Therefore, it is a continuous goal for researchers to develop effective and sensitive detection techniques for Hg^{2+} ions.

In recent years, many efforts have been made for detection, including atomic absorption spectroscopy, inductively coupled plasma-mass spectrometry, high performance liquid chromatography, electrochemical sensing, etc.[7, 8] Among the different detection methods, the use of fluorescence techniques for Hg^{2+} detection has been much appreciated owing to their low detection limit, real-time detection, portability, high selectivity and sensitivity and simple operation procedures.[9-12] Up to now, various fluorescent sensors for selective detection of Hg^{2+} have attracted a surge of attention, especially, "reactive" molecular sensors, i.e. chemodosimeters.[13-25] Compared with coordination-based fluorescent chemosensors,[26] chemodosimeters can not only provide high selectivity towards Hg^{2+} owing to specific mercury-promoted reactions, including desulfurization, oxymercuration, thiol elimination et.al. ,[13, 24, 27-32] but also often exhibit obvious spectroscopic changes that could avoid Hg^{2+} induced fluorescence quenching.[33, 34] Nevertheless they are far from ideal function material, for example, most chemodosimeters based on OFF–ON mechanism just have changes in fluorescence intensity, which can be easily influenced by the excitation power and detector sensitivity.[23, 35-37] By contrast, ratiometric fluorescent chemodosimeters can minimize the background signal by using the ratio of two fluorescent bands, thereby detecting the analyte more accurately.[38-40] Most of these chemodosimeters require a high proportion of organic solvent as the solution for analysis.[21, 41] Furthermore, the majority of these chemodosimeters developed are unrecyclable, because both breaking and forming of the covalent bonds are generally invovled in those mercury-promoted chemical transformations.[42, 43] In addition, rare Hg^{2+} chemodosimeters developed on two-photon fluorescence, which excited by two/multi photons of lower energy and have been widely used in the field of biomedicine.[44, 45]

Recently we devised a novel reaction-based recyclable two-photon fluorescent chemodosimeter **1** for Hg^{2+} in nearly aqueous solution under mild condition. The design strategy was inspired by a specific mercury-promoted reaction,[46] which was constructed with allyl and hydroxy as moiety reaction site, via hampering the excited state intramolecular proton transfer (ESIPT) process between hydroxy and the N atom of benzothiazole. Fortunately, chemodosimeter **1** displayed specific and ratiometric fluorescent response to Hg^{2+}. However, the time of **1** reacting with Hg^{2+} took 2 hours. Further, we designed another chemodosimeter **2**, in which S atom in benzothiazole group is replaced by O atom and the response time is reduced to about 30 min. More importantly, chemodosimeters **1** and **2** both could remove Hg^{2+} from water by forming unique mercury-containing compounds and could be reused in the presence of $NaBH_4$. Moreover, two chemodosimeters had been successfully applied for detecting Hg^{2+} in drinking water with low detection limits (< 2 ppb). Additionally, **1** could be certified as a two-photon chemodosimeter for Hg^{2+} with large two-photon absorption cross section and it could be used for vitro and vivo

imaging.[46]

2. Experimental section

2.1. Materials and general methods

All reagents and solvents were obtained commercially and used without further purification unless otherwise noted. ^{1}H NMR and ^{13}C NMR spectra were recorded on a JEOLBCS 400M spectrometer and referenced to the solvent signals. Mass spectra (ESI) were performed on a LQC system (Finngan MAT, USA). HRMS were performed on an APEX IV (Bruker, USA) mass spectrometer. UV−vis spectra were recorded on a Cary-5000 (Agilent, AUS) spectrophotometer. The melting points were measured on an X-6 melting point apparatus without calibration (Beijing Fuka Keyi Science and Technology Co., LTD).

One-photon fluorescence spectra were recorded using a Hitachi F-7000 spectrofluorometer. All one-photon fluorescence spectra of **1** were measured with an excitation wavelength at 350 nm and **2** were measured with an excitatiwon wavelength at 340 nm. The excitation and emission slit widths of **1** were 2.5 nm and 5.0 nm, respectively, and **2** were 2.5 nm and 2.5 nm, respectively.

Two-photon fluorescence spectra were measured using an Edinburgh FLSP920 equipped with a Xe 700 lamp as the excitation source. The excitation and emission slit widths were 1.0 nm and 1.0 nm, respectively. Two-photon absorption cross sections were measured using the two-photon-induced fluorescence measurement technique. The two-photon absorption cross sections (δ) were determined by comparing their two-photon excitation fluorescence (TPEF) to that of fluorescein in different solvents, according to the following equation:

$$\delta = \delta_{ref} \cdot \frac{n_{ref}}{n} \cdot \frac{\Phi_{ref}}{\Phi} \cdot \frac{c_{ref}}{c} \cdot \frac{F}{F_{ref}}$$

In the equation, the subscript ref stands for the reference molecule. δ is the two-photon adsorption cross-section value, n is the refractive index of the solution, Φ is the fluorescence quantum yield, c is the concentration of solution, F is the TPEF integral intensities of the solution emitted at the exciting wavelength. The δ_{ref} value of reference was taken from the literature.[47] The quantum yields at room temperature were measured by the optically dilute method with an aqueous solution of quinine sulfate (Φ_{em} = 0.546, 1% H_2SO_4) as the standard solution.[48]

The solution of $HgCl_2$, $LiClO_4$, NaCl, KCl, $CaCl_2$, $MgCl_2$, $BaCl_2$, $Al(NO_3)_3$, $CrCl_3$, $MnCl_2$, $FeCl_2$, $CoCl_2$, $NiCl_2$, $CuCl_2$, $ZnCl_2$, $CdCl_2$, $Pb(NO_3)_2$, $AgNO_3$ and $FeCl_3$ were prepared in acetonitrile with a concentration of 10 mM, respectively. $PdCl_2$ was prepared in 1:3 brine-MeOH solutions with a concentration of 10 mM. $AuCl_3$ was prepared in DMSO with a concentration of 10 mM. All the anion solutions were prepared from NaF, NaCl, $NaNO_3$, NaAcO, Na_2SO_4 and Na_2CO_3 in distilled water, with a concentration of 10 mM, respectively.

2.2. TP Fluorescence Imaging

TP fluorescence images of **1** labeled cells and tissues were obtained by exciting the probes with a modelocked titanium-sapphire laser source (Mai Tai DeepSee, 80 MHz, 90 fs) set at wavelength 720 nm with Olympus FV1000 laser confocal microscope IX81 with 60 objective, numerical aperture (NA)=0.4. The images signals at 380-430 nm and 500-550 nm range were collected by internal PMTs in a 12 bit unsigned 1024*1024 pixels at 40 Hz scan speed.

2.3. Synthesis Preparation of chemodosimeter 1

2-(benzo[d]thiazol-2-yl)phenol (5)

This compound was synthesized according to the literature procedure.[49]

2-(2-(allyloxy)phenyl)benzo[d]thiazole (6)

To a solution of 2-(benzo[d]thiazol-2-yl)phenol **5** (1.00 g, 10.0 mmol) in 30 mL acetone was added 3-bromoprop-1-ene (0.70 mL, 20.0 mmol) and K_2CO_3 (1.22g, 20.0 mmol). The mixture was stirred for 2 h at reflux temperature and cooled down to room temperature, inorganic salt was filtrated off. Then the crude product was washed with water and CH_2Cl_2 and dried at 60 °C to afford **6** (1.11 g, 96%). M.p. 47.5 -52.1 °C. ^{1}H NMR (400 MHz, $CDCl_3$) δ 8.53 (dd, J = 7.9, 1.7 Hz, 1H), 8.08 (dd, J = 8.2, 0.7 Hz, 1H), 7.94-7.90 (m, 1H), 7.50-7.45 (m, 1H), 7.43 (ddd, J = 8.3, 7.3, 1.8 Hz, 1H), 7.38-7.34 (m, 1H), 7.12 (ddd, J = 7.8, 7.3, 1.1 Hz, 1H), 7.05 (dd, J = 8.3, 0.7 Hz, 1H), 6.30-6.17 (m, 1H), 5.45 (ddq, J = 52.2, 10.5, 1.4 Hz, 2H), 4.80 (dt, J = 5.5, 1.4 Hz, 2H); ^{13}C NMR (100 MHz, $CDCl_3$) δ 163.31, 156.72, 149.20, 140.06, 136.49, 136.45, 133.84, 128.52, 125.39, 125.32, 125.04, 119.33, 119.25, 116.01, 110.73, 110.20, 34.19. ESI-MS m/z [$(M + H)^+$]: 267.8.

2-allyl-6-(benzo[d]thiazol-2-yl)phenol (1)

6 (1.10 g, 7.5 mmol) was dissolved in N-methylpyrrolidone (10 mL) and refluxed for 10 h at 220 °C under Ar. After evaporation of the solvent, the product was purified with silica gel chromatography, eluted with petroleum ether to afford **1** (0.88 g, 80%). M.p.73.1-75.6 °C. ^{1}H NMR (400 MHz, $CDCl_3$) δ 7.92 (dd, J = 24.6, 7.9 Hz, 1H), 7.58 (dd, J = 7.8, 1.4 Hz, 1H), 7.52-7.45 (m, 1H), 7.44-7.33 (m, 1H), 6.90 (t, J = 7.6 Hz, 1H), 6.08 (ddt, J = 16.8, 10.1, 6.6 Hz, 1H), 5.11 (ddd, J = 9.5, 3.1, 1.6 Hz, 1H), 3.52 (d, J = 6.5 Hz, 1H); ^{13}C NMR (100 MHz, $CDCl_3$) δ 169.78, 155.96, 151.83, 136.57, 133.09, 132.75, 128.90, 126.75, 126.67, 125.56, 122.15, 121.58, 119.28, 116.39, 115.91, 34.27. ESI-MS m/z [$(M + H)^+$]: 267.8.

3. Results and discussion

3.1. Fluorescence response toward Hg^{2+}

The synthetic route to compounds **1** and **2** is shown in scheme 1. Chemodosimeter **1**, 2-allyl-6-(benzo[d]thiazol-2-yl)phenol and chemodosimeter **2**, 2-allyl-6-(benzo[d]- oxazol-2-yl)phenol were prepared smoothly through nucleophilic substitution and rearrangement steps in a satisfactory yield. The structure of **1** and **2** was fully confirmed by ^{1}H, ^{13}C NMR, ESI-MS (Fig. S15-S17, Fig. S21-S23).

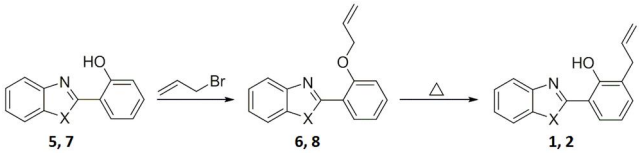

Scheme 1 Synthesis of chemodosimeter **1**, **2**.

First, the fluorescent spectroscopic properties of **1** and **2** were studied. Chemodosimeter **1** (10 μM) exhibited strong fluorescence (λ_{em} = 530 nm, quantum yield, Φ = 0.011) upon excitation at 350 nm in PBS buffer solution (pH = 7.4, containing 0.5% CH_3CN) at room temperature. After treatment with Hg^{2+} (10 μM), the emission at 530 nm decreased, along with an increase in the emission at 401 nm (quantum yield, Φ = 0.023). Accordingly, a fluorescent change from green to blue as well as an emission with a well-defined iso-emissive point at 494 nm was observed (Fig. 1a). Chemodosimeter **2** (10 μM) exhibited strong fluorescence emission in aqueous solution (containing 0.5% CH_3CN) at 508 nm (quantum yield, Φ =0.058) at room temperature. After adding Hg^{2+} (10 μM), the emission at 508 nm decreased, along with an increase in the emission at 390 nm (quantum yield, Φ =0.164), with an isosbestic point at 480 nm (Fig. 1b). The remarkable blue shift is due to hamper the excited state intramolecular proton transfer (ESIPT) process and form the mercury compound.

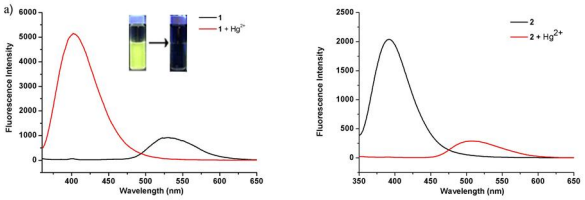

Fig. 1 a) Fluorescence spectral change of **1** (10 uM) upon treatment with $HgCl_2$ (10 uM) in PBS buffer solution (pH = 7.4, containing 0.5% CH_3CN). λ_{ex} = 350 nm. Slit: 2.5 nm/5.0 nm. Inset: the fluorescent change in **1** (10 uM) upon addition of Hg^{2+} (10 uM) under UV lamp. b) Fluorescence spectral change of **2** (10 uM) upon treatment with $HgCl_2$ (10 uM) in aqueous solution (containing 0.5% CH_3CN). λ_{ex} = 340 nm. Slit: 2.5 nm/2.5 nm.

When 1 equiv. of $HgCl_2$ was added to **1** in aqueous solution, the fluorescence saturation took about 2 hours (Fig. S1). By contrast, the fluorescence saturation of **2** only took 30 min (Fig. S2). The fluorescence saturation of **1** in PBS buffer took about 4 hours (Fig. S3).

3.2. Ion Selectivity and Competitiveness

In order to evaluate a practical applicability of **1** for Hg^{2+} sensing, the interference of other ions should be excluded. Therefore, the fluorescence spectrum of **1** was measured in the presence of respective metal cations including Li^+, Na^+, K^+, Ca^{2+}, Mg^{2+}, Ba^{2+}, Al^{3+}, Cr^{3+}, Mn^{2+}, Fe^{2+}, Co^{2+}, Ni^{2+}, Cu^{2+}, Zn^{2+}, Cd^{2+}, Au^{3+}, Pd^{2+}, Pb^{2+}, Ag^+ and Fe^{3+} under identical conditions. After incubating **1** (10 μM) with metal ions (10 μM) individually for 30 min, the results showed that these ions had negligible response to the emission of **1** (Fig. 2a). To further explore the selectivity of Hg^{2+} in the presence of other metal ions, the competition experiments were conducted in the presence of 1 equiv. of Hg^{2+} mixed with different mental ions (1 equiv.), which showed these metal ions almost had little interference on the sensing of Hg^{2+} (Fig. 2b). Moreover, as shown in Fig. S5a, after addition of 1.0 equiv of anions such as F^-, Cl^-, NO_3^-, AcO^-, CO_3^{2-} and SO_4^{2-} under the established conditions, both **1** and **1**-Hg^{2+} system showed little response to these anions. These results indicate that **1** shows a good sensitivity and selectivity towards Hg^{2+} over other competitive ions. The competition experiments and selectivity experiments of **2** were also conducted as the method above. The results showed that the fluorescence profiles of **2** and **2**-Hg^{2+} were almost not affected by other ions (Fig S4, Fig S5b).

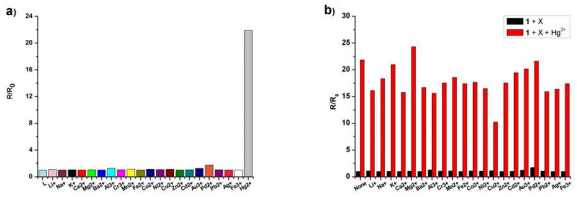

Fig. 2 a) Fluorescence spectra of **1** in the absence and presence of different metal ions Li^+, Na^+, K^+, Ca^{2+}, Mg^{2+}, Ba^{2+}, Al^{3+}, Cr^{3+}, Mn^{2+}, Fe^{2+}, Co^{2+}, Ni^{2+}, Cu^{2+}, Zn^{2+}, Cd^{2+}, Au^{3+}, Pd^{2+}, Pb^{2+}, Ag^+, Fe^{3+} and Hg^{2+} in PBS buffer solutions (pH = 7.4, containing 0.5% CH_3CN). b) Changes in fluorescence of **1** (10 uM) upon addition of Hg^{2+} (1 equiv.) with various mental ions (1 equiv.). Bars represent the fluorescence intensity ratio in the presence (R) and absence (R_0) of various mental ions. λ_{ex} = 350 nm. Slit: 2.5 nm/5.0 nm; R = $I_{401\ nm}/I_{494\ nm}$. Each spectrum was acquired 30 min after mental ions addition.

3.3. Sensing mechanism

To gain insight into the sensing mechanism of **1** and **2** towards Hg^{2+}, the reaction products **1** and **2** were obtained and characterized to be **3** and **4** respectively by ^1H NMR, ^{13}C NMR and HRMS (Fig. S24-S29). Then, we further explored the reversibility of **1** and **2** by measuring the fluorescence changes in situ upon reacting with Hg^{2+} and $NaBH_4$ for several cycles (Fig 3, S6). We found that, after four cycles, **1** still showed excellent reversibility with little fluorescent efficiency loss (Fig 3) and after three cycles, **2** still showed excellent reversibility (Fig S6). The reversible cycle process was also proved by in situ NMR titration experiments (Fig. S30, S31). It showed that, with addition of Hg^{2+}, the hydroxy peak disappeared and the peaks of methyl of the methylmercury group appeared simultaneously. Then, upon addition of $NaBH_4$, the hydroxy peak appeared and the chemical shifts were identical with chemodosimeters. This realized the ability to recycle the chemodosimeters and it is quite important for chemodosimeters considering their non-reversibility. Moreover, the results obtained from Job's plot also show that the 1:1 stoichiometry for the reaction between the chemodosimeters and Hg^{2+} (Fig. S7) .[50, 51] Thus, the mechanism can be explained by the procedure in Scheme 2. Furthermore, the results indicate that **1** and **2** can not only detect Hg^{2+}, but also remove Hg^{2+} from water.

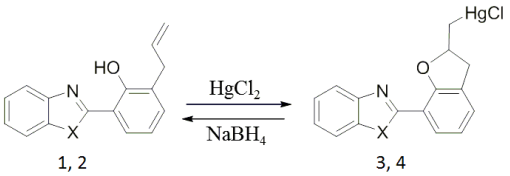

1, 2 3, 4

1, 3, X = S

2, 4, X = O

Scheme 2 Graphic of proposed mechanism of the sensing system.

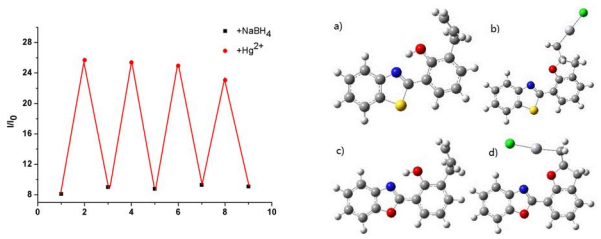

Fig. 3 The reversibility of **1** (10 μM) reacting with Hg^{2+} (10 μM) in PBS buffer solution (pH = 7.4, containing 0.5% CH_3CN). The spectrum was acquired 30 min after Hg^{2+} addition. Calculated energy-minimized structure of a) **1**, b) **1**-Hg^{2+}, c) **2**, d) **2**-Hg^{2+}. The gray, blue, red, yellow, green, silver and light gray colors denote C, N, O, S, Cl, Hg and H atoms respectively.

Furthermore, the optimized configuration of **1**, **1**-Hg^{2+}, **2** and **2**-Hg^{2+} was calculated by Density Functional Theory (DFT). As seen from Fig. 3, the distances between the H of hydroxy and the N in **1** and **2** are 1.740 Å and 1.779 Å respectively, satisfing the excited state intramolecular proton transfer (ESIPT) happening condition.[52] However, the mercury compounds **1**-Hg^{2+} and **2**-Hg^{2+} form five-membered rings via the reactions between allyl and hydroxy and hamper the ESIPT process.

3.4. Fluorescence Titration

Detection of Hg^{2+} in water is of great importance since it is very toxic. When different concentrations of Hg^{2+} (0-10 μM) were added to **1** (10 μM) in PBS buffer solution, the fluorescence spectrum was acquired 30 min after the addition of Hg^{2+}. The emission intensity ratios (I_{401} nm/I_{494} nm) increased with increasing Hg^{2+} concentration (Fig 4a). **2** was also detected as the method above in aqueous solution (containing 0.5% CH_3CN) and exhibited a good linear relationship (Fig S8a, $R^2 = 0.9962$).

Moreover, in drinking water, good linear relationship (R_1^2 = 0.9924, R_2^2 = 0.9889) could also be found between the fluorescence intensity ratios and the low concentration range of Hg^{2+} (0-2 μM) (Fig 4b, S8b). The detection limit of **1** for Hg^{2+} was calculated to be 5.1 nM (Hg content = 1.0 ppb); the detection limit of **2** for Hg^{2+} was calculated to be 3.8 nM (Hg content = 0.7 ppb). They are all lower than many reported results [21, 24, 43] and satisfy the U.S. Environmental Protection Agency (EPA) limits (~ 2 ppb) of Hg^{2+} detection in drinking water.

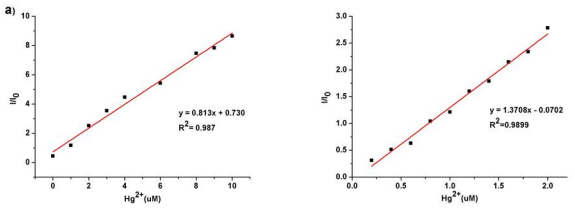

Fig. 4 a) The linear relationship of **1** between the concentration of Hg^{2+} within the range 0-10 μM and the fluorescence intensity ratios at 401 nm and 494 nm (I_{401nm}/I_{494nm}) in PBS buffer solution (pH = 7.4, containing 0.5% CH_3CN). b) The linear relationship of **1** between Hg^{2+} concentration within the range 0-2 μM and the fluorescence intensity ratios (I_{401nm}/I_{494nm}) in drinking water.

3.5. Two-photon properties and its Application in Bioimaging

3.5.1 Two-photon Absorbtion Cross Section (δ)

We studied the responses between the chemodosimeters and Hg^{2+} use the two-photon induced fluorescence measurement technique. The two-photon (TP) cross sections and the normalized TP fluorescence intensity of chemodosimeters and their Hg^{2+} complexes were measured. As shown in Fig. S9a, **1** shows the δ_{max} value of 103.8 GM at 720 nm; and its Hg^{2+} complex shows the δ_{max} value of 160.1 GM at 700 nm. The TP cross sections of **2** and its Hg^{2+} complex are shown in Fig. S9b, **2** shows the δ_{max} value of 261.8 GM at 700 nm, its Hg^{2+} complex exhibits weak two-photon action cross sections < 40 GM, which is lower than **1**-Hg^{2+}. So **1** is more satisfied to be a ratiometric TP fluorescence chemodosimeter for Hg^{2+} in the living systems.

3.5.2 Cell Cytotoxicity

The pH effect on the fluorescence of **1** and **1**-Hg^{2+} system has been studied. It was found that **1** is pH insensitive between pH 4.95 and 9.05, and it reacted faster with Hg^{2+} within the biological relevant pH range (7.07 ~ 7.93) (Fig S10). So, it could be used in biological analysis wonderfully.[46] To further demonstrate the ability of **1** to image Hg^{2+} ions in living systems, we carried out imaging experiments in HeLa cells. Firstly, we studied the cell viability of compound probe **1** and **1**-Hg^{2+} complex using the MTT assay. As seen from Fig S11, the HeLa cells displayed high viability as the concentration of **1** increased from 10 μM to 100 μM, and with the added equal amount of Hg^{2+} increased and the activity of HeLa cells declined. Amazingly, although the concentration of the **1** and **1**-Hg^{2+} were 50 μM respectively, the viability of HeLa cells was still over 60%. And we selected the testing amount was 10 μM, which just had negligible toxicity to the cells. The results suggest that **1** exhibits low toxicity to HeLa cells in our measure range and could be used to detect Hg^{2+} in vivo with little damage.

3.5.3 TP Bioimaging

Then we utilized the two-photon fluorescence microscopy experiment technique to investigate its higher gradation of application in complex biological systems. Data in Fig. 5 showed that after incubated for 30 min in a CO_2 incubator, the cells incubated with 10 μM **1** exhibited green fluorescence when induced by TP excitation light source (Fig. 5d). However, when the cells were treated with 10 μM **1** and 10 μM $HgCl_2$, they displayed blue fluorescence (Fig. 5h). Obvious changes indicated that **1** could penetrate the cell membrane and enable ratiometric imaging of Hg^{2+} in the living cells with no autofluorescence and high resolution.

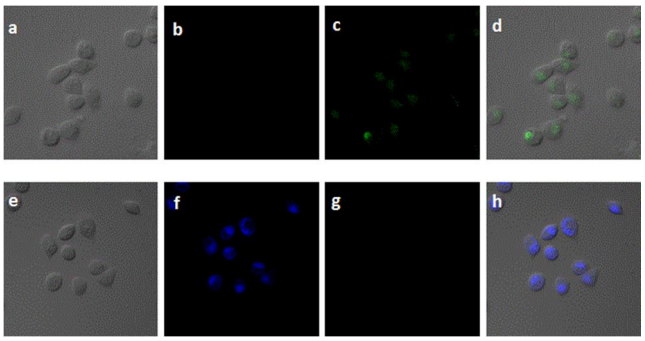

Fig. 5 Images of HeLa cells incubated with 10 μM **1** for 30 min (up); images of HeLa cells incubated with 10 μM **1** for 30 min and then further incubation with 10 μM $HgCl_2$ for 1.0 h (down). Bright-field images (a, e), TP microscope images using blue channel (b, f), TP microscope images using green channel (c, g) and the overlay of fluorescence and bright-field images (d, h) of HeLa cells.

Also, we studied the quantitative determination property of **1** to Hg^{2+} in the living cells. When the concentration of Hg^{2+} reached to 1.5 μM, observable fluorescence was appeared and the blue fluorescence intensity increased with increasing Hg^{2+} concentration until 10 μM (Fig. 6). As expected, the relationship of intensity and the concentration of Hg^{2+} exhibited an excellent linear relationship in the range of 0-10 μM (Fig. 6) using the software Imagepro-plus, which could calculate the average fluorescence intensity and quantify the images. So the chemodosimeter **1** can not only detect Hg^{2+} in the living cells qualitatively, but also detect the Hg^{2+} concentration quantitatively in vivo. As far as we known, this is the first quantitative determination chemodosimeter for Hg^{2+} in vivo.

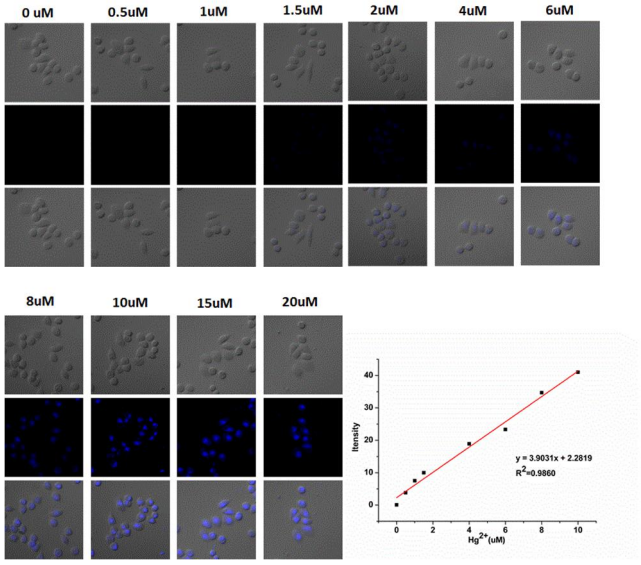

Fig. 6. Bright-field images (up), TP microscope images (middle), and the overlay of fluorescence and bright-field images (down) of HeLa cells after incubation with 10 μM **1** for 30 min and then further incubated with 0-20 μM Hg^{2+} for another 1 h. And the relationship between average fluorescence intensity and Hg^{2+} concentration (0-10 μM).

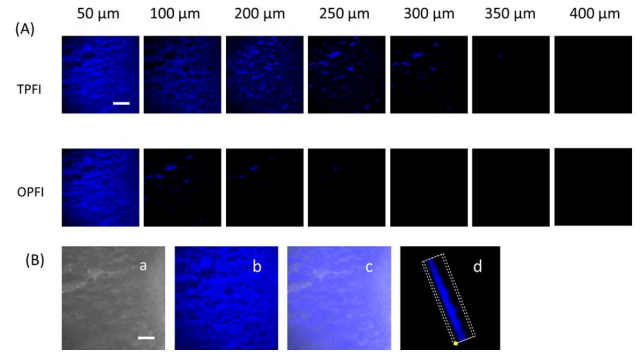

Fig. 7. The confocal fluorescence imaging of a part of a fresh thick cervical tissue slice stained by **1**. (A) Z-scan TPE (TPFI) and OPE (OPFI) fluorescence images at different penetration depths, the scale bar is 80 μm; (B) Bright-field image (a), TPE fluorescence image (b), overlay image (c) and the 3D reconstruction from 50 confocal Z-scan TPE imaging sections at depth of 0-500 μm with 60×magnification, the scale bar is 60 μm.

The superiority of TP over OP (one-photon) is that the penetration depth of TP is deeper than that of OP, and it was proved perfectly by the fluorescence images experiments of labeled tissues. As shown in Fig. 7, when certain concentration of **1** and Hg^{2+} were added into the tissues, very strong blue-fluorescence was presented whether it was excited by OP or TP. We can still observe that the penetration depth of fluorescence from TP fluorescence microscope could reach to 300 μm; however, it was only up to 200 μm from OP fluorescence microscope. Above all, **1** is capable of detecting Hg^{2+} in tissues by using TPM.

4. Conclusion

In conclusion, we have developed two new recyclable fluorescent chemodosimeters for detection of Hg^{2+}. The chemodosimeters display specific and ratiometric fluorescent response towards Hg^{2+} with low detection limits (< 2 ppb). Moreover, the chemodosimeters can remove Hg^{2+} from water by forming mercury-containing compounds and the chemodosimeters could be recycled with addition of $NaBH_4$. Furthermore, **1** can be used as a ratiometric TP fluorescence chemodosimeter to imaging of Hg^{2+} in living cells and tissues with low cytotoxicity and autofluorescence. Besides, it can detect the Hg^{2+} concentration quantitatively in vivo utilizing TP bioimaging technique.

Acknowledgments

This study was supported by the NSFC (Grant 91122007 and 21431002) and the Specialized Research Fund for the Doctoral Program of Higher Education (Grant No. 20110211130002).

Notes and references

Key Laboratory of Nonferrous Metals Chemistry and Resources Utilization of Gansu Province and State Key Laboratory of Applied Organic Chemistry, College of Chemistry and Chemical Engineering, Lanzhou University, Lanzhou 730000, P. R. China

** Corresponding authors. Tel.: +86 931 8915151; fax: +86 931 8912582*

E-mail addresses: liuws@lzu.edu.cn (W. S. Liu)

† Electronic Supplementary Information (ESI) available: [details of any supplementary information available should be included here]. See DOI: 10.1039/b000000x/

[1] J. Gutknecht, *J. Membr. Biol.*, 1981, **61**, 61-66.
[2] R. Von Burg, *J. Appl. Toxicol.*, 1995, **15**, 483-493.
[3] M. A. Palacios, Z. Wang, V. A. Montes, G. V. Zyryanov and P. J. Anzenbacher, *J. Am. Chem. Soc.*, 2008, **130**, 10307-10314.
[4] T. W. Clarkson, L. Magos and G. J. N. Myers, *N. Engl. J. Med.*, 2003, **349**, 1731-1737.
[5] E. L. Que, D. W. Domaille and C. J. Chang, *Chem. Rev.*, 2008, **108**, 1517-1549.
[6] World Health Organization, Guidelines for drinking-water quality, *Geneva*, 2004, **1**, 188.
[7] Y. Li, C. Chen, B. Li, J. Sun, J. Wang, Y. Gao, Y. Zhao and Z. Chai, *J. Anal. At. Spectrom.*, 2006, **21**, 94-96.
[8] O. T. Butler, J. M. Cook, C. F. Harrington, S. J. Hill, J. Rieuwerts and D. L. Miles, *J. Anal. At. Spectrom.*, 2006, **21**, 217-243.
[9] X. Chen, X. Tian, I. Shin and J. Yoon, *Chem. Soc. Rev.*, 2011, **40**, 4783-4804.
[10] D.-G. Cho and J. L. Sessler, *Chem. Soc. Rev.*, 2009, **38**, 1647-1662.
[11] A. Razgulin, N. Ma and J. Rao, *Chem. Soc. Rev.*, 2011, **40**, 4186-216.
[12] H. N. Kim, M. H. Lee, H. J. Kim, J. S. Kim and J. Yoon, *Chem. Soc. Rev.*, 2008, **37**, 1465-1472.
[13] M. Y. Chae and A. W. Czarnik, *J. Am. Chem. Soc.*, 1992, **114**, 9704-9705.
[14] Y. Zhao and Z. Zhong, *J. Am. Chem. Soc.*, 2006, **128**, 9988-9989.
[15] X. Peng, Y. Wang, X. Tang and W. Liu, *Dyes Pigm.*, 2011, **91**, 26-32.
[16] H. N. Kim, W. X. Ren, J. S. Kim and J. Yoon, *Chem. Soc. Rev.*, 2012, **41**, 3210-3244.

[17] M. Ghanei-Motlagh, M. Fayazi and M. A. Taher, *Sens. Actuators B*, 2014, **199**, 133-141.
[18] A. A. Abdel Aziz and S. H. Seda, *Sens. Actuators B*, 2014, **197**, 155-163.
[19] X. Ma, J. Wang, Q. Shan, Z. Tan, G. Wei, D. Wei and Y. Du, *Org. Lett.*, 2012, **14**, 820-823.
[20] W. Xuan, C. Chen, Y. Cao, W. He, W. Jiang, K. Liu and W. Wang, *Chem. Commun.*, 2012, **48**, 7292-7294.
[21] F. Lu, M. Yamamura and T. Nabeshima, *Dalton Trans.*, 2013, **42**, 12093-12100.
[22] B. Tang, B. Ding, K. Xu and L. Tong, *Chem. Eur. J.*, 2009, **15**, 3147-3151.
[23] J. Du, J. Fan, X. Peng, P. Sun, J. Wang, H. Li and S. Sun, *Org. Lett.*, 2010, **12**, 476-479.
[24] F. Wang, S.-W. Nam, Z. Guo, S. Park, J. Yoon, *Sens. Actuators B*, 2012, **161**, 948-953.
[25] T. Q. Duong and J. S. Kim, *Chem. Rev.*, 2010, **110**, 6280-6301.
[26] R. Martínez-Máñez and F. Sancenón, *Chem. Rev.*, 2003, **103**, 4419-4476.
[27] X. Cheng, S. Li, A. Zhong, J. Qin and Z. Li, *Sens. Actuators B*, 2011, **157**, 57-63.
[28] V. R. Jose, M. D. Marcos, M. M. Ramon, K. Rurack and J. Soto, *Angew. Chem. Int. Ed.*, 2005, **44**, 4405-4407.
[29] M. H. Lee, S. W. Lee, S. H. Kim, C. Kang and J. S. Kim, *Org. Lett.*, 2009, **11**, 2101-2104.
[30] S. Park, W. Kim, K. M. K. Swamy, H. Y. Lee, J. Y. Jung and G. Kim, *Dyes Pigm.*, 2013, **99**, 323-328.
[31] M. G. Choi, D. H. Ryu, H. L. Jeon, S. Cha, J. Cho and S. K. Chang, *Org. Lett.*, 2008, **10**, 3717-3720.
[32] M. E. Jun, B. Roy and K. H. Ahn, *Chem. Commun.*, 2011, **47**, 7583-7601.
[33] Y.-Y. Guo, X.-L. Tang, F.-P. Hou, J. Wu, W. Dou and W.-W. Qin, *Sens. Actuators B*, 2013, **181**, 202-208.
[34] M. J. Culzoni, A. Munoz de la Pena, A. Machuca, H.C. Goicoechea and R. Babiano, *Anal. Methods*, 2013, **5**, 30-49.
[35] D. Srikun, E. W. Miller, D. W. Domaille and C. J. Chang, *J. Am. Chem. Soc.*, 2008, **130**, 4596-4597.
[36] Q. Li, M. Peng, H. Li, C. Zhong, L. Zhang, X. Cheng, X. Peng, Q. Wang, J. Qin and Z. Li, *Org. Lett.*, 2012, **14**, 2094-2097.
[37] B. Gao, W.-T. Gong, Q.-L. Zhang, J.-W. Ye, G.-L. Ning, *Sens. Actuators B*, 2012, **162**, 391-395.
[38] Z. Xu, K.-H. Baek, H. N. Kim, J. Cui, X. Qian, D. R. Spring, I. Shin and J. Yoon, *J. Am. Chem. Soc.*, 2010, **132**, 601-610.
[39] D. W. Domaille, L. Zeng and C. J. Chang, *J. Am. Chem. Soc.*, 2010, **132**, 1194-1195.
[40] X. Cheng, Q. Li, J. Qin and Z. Li, *ACS Appl. Mater. Interfaces*, 2010, **2**, 1066- 1072.
[41] A. K. Atta, S.-B. Kim, J. Heo and D.-G. Cho, *Org. Lett.*, 2013, **15**, 1072-1075.
[42] H. B. Yu, M. Y. Fu and Y. Xiao, *Phys. Chem. Chem. Phys.*, 2010, **12**, 7386-7391.
[43] R. Koteeswari, P. Ashokkumar, E. J. Padma Malar, V. T. Ramakrishnan and P. Rama-murthy, *Chem. Commun.*, 2011, **47**, 7695-7697.
[44] J. F. Zhang, C. S. Lim, B. R. Cho and J. S. Kim, *Talanta.*, 2010, **83**, 658-662.
[45] X. Zhang, X.-J. Huang and Z.-J. Zhu, *RSC Adv.*, 2013, **3**, 24891-24895.
[46] W.-T. Gong, B. Gao, J.-Z. Zhao and G.-L. Ning, *J. Mater. Chem. A*, 2013, **1**, 5501-5504.
[47] M. A. Albota, C. Xu and W. W. Webb, *Applied Optics*, 1998, **37**, 7352-7356.
[48] J. N. Demas and G. A. Crosby, *J. Phys. Chem.*, 1971, **75**, 991–1024.
[49] E. Barni, P. Savarino, M. Marzona and M. Piva, *J. Heterocyclic. Chem.*, 1983, **20**, 1517-1521.
[50] H. Wang, G. Zhou, H. Gai and X. Chen, *Chem. Commun.*, 2012, **48**, 8341-8343.
[51] J. Shi, Y. Wang, X. Tang, W. Liu, H. Jiang and W. Dou, *Dyes Pigm.*, 2014, **100**, 255-260.
[52] H. Kobayashi, O. Mikako, A. Raphael, L. C. Peter and U. Yasuteru, *Chem. Rev.*, 2010, **110**, 2620-2640.

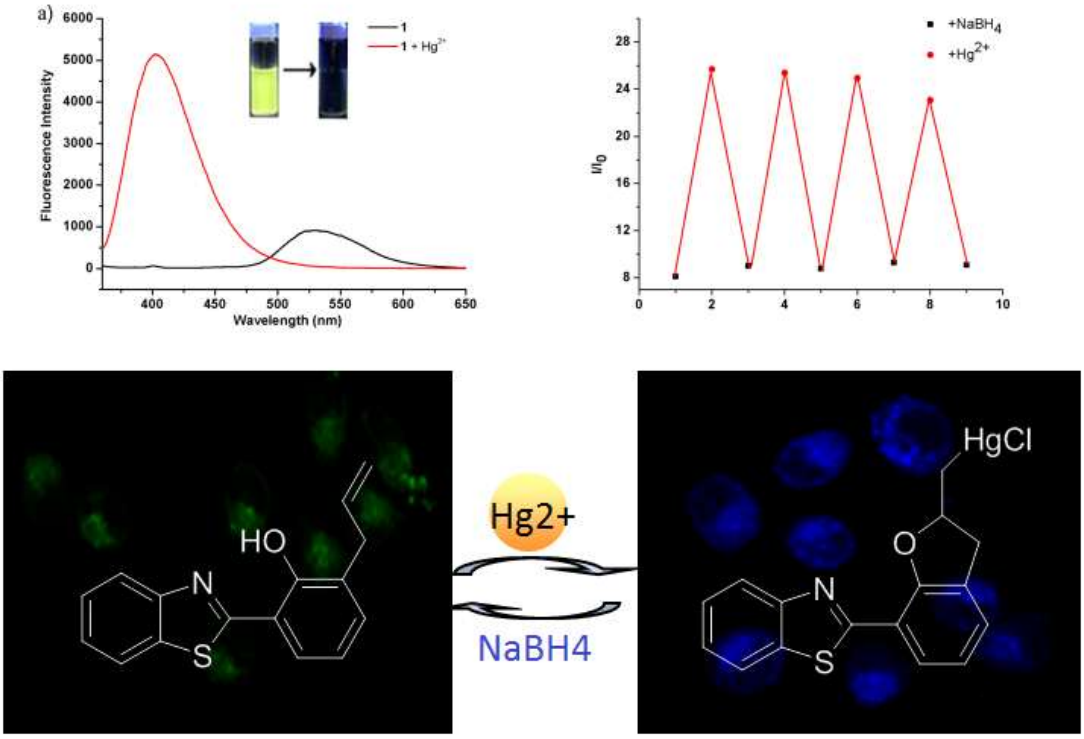

A novel reaction-based recyclable two-photon chemodosimeter for Hg^{2+} in nearly aqueous solution and it could be used for bioimaging.